Biological Psychology 114 (2016) 69–80

Contents lists available at ScienceDirect

Biological Psychology

journal homepage: www.elsevier.com/locate/biopsycho

Genetic effects on source level evoked and induced oscillatory brain responses in a visual oddball task

Marios Antonakakis[a,*], Michalis Zervakis[a], Catharina E.M. van Beijsterveldt[b], Dorret I. Boomsma[b,c], Eco J.C. De Geus[b,c], Sifis Micheloyannis[a,d], Dirk J.A. Smit[b,c,1]

[a] School of Electronic and Computer Engineering, Technical University of Crete, Chania 73100, Greece
[b] Biological Psychology, VU University, van der Boechorststraat 1, 1081 BT Amsterdam, The Netherlands
[c] Neuroscience Campus Amsterdam, VU University, De Boelelaan 1085, 1081 HV Amsterdam, The Netherlands
[d] Faculty of Medicine, University of Crete, Heraklion 71110, Greece

ARTICLE INFO

Article history:
Received 11 December 2014
Received in revised form
28 November 2015
Accepted 22 December 2015
Available online 29 December 2015

Keywords:
Twin study
Heritability
EEG
ICA
P300
Time-frequency analysis
Endophenotype

ABSTRACT

Stimuli in simple oddball target detection paradigms cause evoked responses in brain potential. These responses are heritable traits, and potential endophenotypes for clinical phenotypes. These stimuli also cause responses in oscillatory activity, both evoked responses phase-locked to stimulus presentation and phase-independent induced responses. Here, we investigate whether phase-locked and phase-independent oscillatory responses are heritable traits. Oscillatory responses were examined in EEG recordings from 213 twin pairs (91 monozygotic and 122 dizygotic twins) performing a visual oddball task. After group Independent Component Analysis (group-ICA) and time-frequency decomposition, individual differences in evoked and induced oscillatory responses were compared between MZ and DZ twin pairs. Induced (phase-independent) oscillatory responses consistently showed the highest heritability (24–55%) compared to evoked (phase-locked) oscillatory responses and spectral energy, which revealed lower heritability at 1–35.6% and 4.5–32.3%, respectively. Since the phase-independent induced response encodes functional aspects of the brain response to target stimuli different from evoked responses, we conclude that the modulation of ongoing oscillatory activity may serve as an additional endophenotype for behavioral phenotypes and psychiatric genetics.

1. Introduction

Twin studies may be used to investigate genetic influences on individual differences in biological and behavioral traits (Ehringer, Rhee, Young, & Corley, Hewitt, 2006; van Dongen, Slagboom, Draisma, Martin, Boomsma, 2012; Anokhin, 2014), including psychophysiological measures linked to liability of psychopathology (e.g., van Beijsterveldt and van Baal, 2002; Ehringer et al., 2006; Smit, van Ent, Zubicaray, & Stein, 2012; Ethridge, Malone, Iacono, & Clementz, 2013). Studies assessing endophenotypes—i.e., intermediate phenotypes in the expression pathway from genes to phenotype (Gottesman and Gould, 2003)—found that many electroencephalographic (EEG–based) endophenotypes are to some extent genetically determined (e.g., O'Connor, Morzorati, Christian, & Li, 1994; Almasy et al., 1999; Smit, Posthuma, Boomsma, & de Geus, 2007; De Geus, 2010; Anokhin, 2014). Of these, the P300 may be the most commonly investigated parameter. This signal is typically elicited in simple visual or auditory "oddball" tasks when the subject is required to distinguish between frequent and rare stimuli present in random series, to respond (or count) the rare target stimulus, while ignoring the frequent nontarget stimulus (Polich and Herbst, 2000). The amplitude of the P300 is modulated by changing the task specifications, e.g., making the target rarer (Kok, 2001). Moreover, the amplitude of the P300 response is altered in alcoholism, schizophrenia, and Alzheimer's disease (Mathalon, Ford, & Pfefferbaum, 2000; Polich and Bloom 1999; Polich and Ochoa 2004; Polich and Corey-Bloom 2005; Ford, 1999; see Polich and Corey-Bloom 2005; Ford 1999; Porjesz et al., 2005 for overviews), which suggests that the P300 amplitude is a biomarker for the cognitive symptoms present in these psychiatric phenotypes (Ford et al., 1994).

Studies of the P300 response in the oddball task have calculated the evoked response by averaging the EEG scalp potentials in time windows relative to the stimulus onset. They thus assess

* Corresponding author.
E-mail addresses: mantonakakis@isc.tuc.gr, antonakakismar@gmail.com (M. Antonakakis).
[1] Contributed equally.

http://dx.doi.org/10.1016/j.biopsycho.2015.12.006
0301-0511/

voltage changes that are time-locked to the event of interest, that is, the rare target stimulus. By averaging across a large number of EEG epochs, ongoing brain activity—pre- and post-stimulus oscillations with phase independent from stimulus events—cancels out in the long run, increasing the relative strength of stimulus-evoked potentials. These event-related potentials (ERPs) consist of a series of positive and negative peaks occurring at a fixed time relative to the event (Ergen, Marbach, Brand, Başar-Eroglu, & Demiralp, 2008; Gilmore, Malone, Bernat, & Iacono, 2010; Ucles, Mendez, & Garay, 2009). The procedure assumes that ongoing oscillatory EEG activity are background "noise" in which the ERP "signal" is embedded. However, oscillations in EEG activity may also carry dynamic information associated with the neural system that generates them in the form of modulation of the oscillatory activity. This modulation may consist of amplitude increase or decrease, and/or a phase-reset resulting in phase-locking to the stimulus event (Makeig et al., 2002; Nikulin et al., 2007). Part of the ERP response may consists of the phase-reset of ongoing oscillations as these will show up in the averaged response (Makeig et al., 2002; Nikulin et al., 2007). Thus, evoked responses phase-locked to the stimulus event may include both evoked potentials (ERPs) and phase-locked oscillatory responses. On the other hand, induced responses are phase-independent oscillatory amplitude modulations (Shah et al., 2004; Mazaheri & Jensen, 2006; David, Kilner, & Friston, 2006) not visible in the ERP. Here, it is our aim to investigate both types of responses in the oddball task.

A comparison of evoked responses with induced response in the alpha band revealed that they are both present in simple stimulus paradigms and both respond to oddball task manipulations. Interestingly, however, both also seem to reflect different aspects of the brain response to the event (Zervakis, Michalopoulos, Iordanidou, & Sakkalis, 2011; Yordanova, Kolev, & Polich, 2001; Klimesch 1999), suggesting they serve different functional roles in stimulus processing related to specific processing steps in the performance of a task even though they resulted from common cognitive events such as target stimulus presentation (Jung et al., 2001; Makeig et al., 2002; Tallon-Baudry, Bertrand, Delpuech, & Pernier, 2002). Evoked oscillatory response can be determined using Phase Intertrial Coherence (PIC) (Jervis et al., 2007; Tallon-Baudry et al., 1996). Combining phase and amplitude into a phase vector, PIC measures the uniformity of distribution of angles weighted by the relative amplitudes of oscillations (Jervis et al., 2007; Tallon-Baudry et al., 1996), yielding large values when all trials are phase-locked to the same phase shift of a specific frequency. A metric revealing the induced response (phase-independent activity) is the Phase shift Intertrial Coherence (PsIC) (Zervakis et al., 2011), which compares the inter-trial consistency of a component in terms of its energy, irrespective of phase relation to the inducing event. In essence, PsIC captures both phase and phase-independent activity by adding up the spectral energy of oscillatory signals. Finally, Spectral Energy (SE) is a measure which captures the (squared) amplitude of each oscillation frequency of the average response over trials, and is therefore the most closely related to the ERP (Jervis et al., 2007; Onton and Makeig, 2006; Tallon-Baudry et al., 1996). Note that both PIC and SE capture phase-locked responses, however, they differ in the sense that the former (PIC) detects phase-locked patterns of oscillatory activity across trials while the latter (SE) determines the spectral energy of intertrial average; in this form, SE can reveal increased energy due to only a small number of individual trials without necessarily indicating consistency of signal peaks across trials.

The P300 evoked potential was found to be associated with many disease phenotypes such as schizophrenia, alcoholism, and Alzheimer's disease (Polich and Bloom 1999; Polich and Ochoa 2004; Polich and Corey-Bloom, 2005; Porjesz et al., 2005; Ford et al., 1994). It may be hypothesized that oscillatory responses are similarly useful biomarkers of brain pathology. Indeed, Alzheimer's disease has been found to lead to reduced evoked oscillatory response (Jeong, 2004; Karrasch et al., 2006; Zervakis et al., 2011) but an absence of induced response (Zervakis et al., 2011; Krause et al., 2000) compared to control state. Schizophrenia (SZ) is associated with reduced evoked oscillatory response (Ford et al., 2008; Brockhaus-Dumke et al., 2007) and substantial reductions of induced response (Bates, Kiehl, Laurens, & Liddle, 2009; Doege, Jansen, Mallikarjun, Liddle, & Liddle, 2010) in patients. Gilmore and Fein (2012) showed that an increased evoked response of theta oscillations in EEG activity was present in long-term abstinent alcoholics (Gilmore and Fein, 2012). In developmental dyslexia (Soltez et al., 2013) the strength of inter-trial delta phase coherence (an evoked oscillatory response) is significantly weaker in dyslexics, suggestive of weaker entrainment and less preparatory brain activity. Gilmore, Malone, Bernat et al. (2010) showed that the oscillatory responses to an oddball stimulus predicted externalizing disorders better than the time-domain evoked potential. As low as six principal components explained most of the variation in the evoked oscillatory response, and combined they carried all or most of the variation present in the evoked potential.

Because of its potential as an endophenotype, many studies have investigated the heritability of the P300 (see De Geus, 2010 and Anokhin, 2014 for overviews). Using the classical twin design (Smit et al., 2010; van Beijsterveldt, Molenaar, de Geus, & Boomsma, 1998) and family studies (Porjesz and Begleiter, 2003), it was found that both amplitude and latency of the P300 wave are heritable traits. A meta-analysis (van Beijsterveldt and van Baal, 2002) found that respectively 60% and 51% of the trait variance could be attributed to additive genetic factors. In spite of their association with disease and the evidence presented above that they provide additional information to and reflect different aspects of stimulus processing than the P300, the heritability of oscillatory responses measured by PIC, PsIC and SE have not been subjected to comparable extensive study (Smit, Stam, Posthuma, Boomsma, & de Geus, 2008; Gilmore, Malone, Bernat et al., 2010; Gilmore, Malone, & Iacono, 2010; Ethridge et al., 2013). A few existing studies used time-frequency analysis (TF) similar to PIC, PsIC and SE (Gilmore, Malone, Bernat et al., 2010, Malone, Iacono et al., 2010; Ethridge et al., 2013). Gilmore, Malone, Iacono et al. (2010) showed that principal components from evoked oscillatory responses were highly heritable, while Gilmore, Malone, Bernat et al. (2010) showed that these were promising endophenotype for various externalizing psychopathologies. The multivariate genetic analysis suggested that the time-frequency analysis of the evoked response carries multiple, partly independent sources of information, supporting the idea that TF analysis. Ethridge et al. (2013) demonstrated that the TF response to oddball stimuli can be parsed into genetic components that largely fit into standard frequency bands. The components for the slower oscillation frequencies (including alpha and lower beta) showed strong genetic effects.

A major goal here is to investigate the genetic or environmental etiology of the induced response to the oddball stimulus. The previous studies examining heritability of the TF response used principal components analysis (PCA) to extract components. PCA does not assume any generative model of the data like source modeling does, and as such is restricted to explaining variance irrespective of the neurogenerative specifics of EEG generation. On the other hand, Independent Component Analysis (ICA) (Onton and Makeig, 2006) can be seen as expanding the potential of PCA, and is highly suitable for non-Gaussian neural generators with fixed position and near immediate responses on scalp-recorded signals (Hyvärinen, 2001; James and Hesse, 2005). ICA is a well-established tool for identifying source-space signals (Onton and Makeig, 2006), to extract oscillatory sources and subject these to TF analysis. Since the application of individual ICA creates different scalp topographies for each subject that are difficult a compare across subjects. Compa-

rability across subjects may be Group ICA, however, estimates a common mixing matrix (i.e., the same mixing matrix for all the subjects) by applying ICA on a merged data matrix concatenating all EEG recordings in order to increase the temporal size of the input to ICA data (Grin-Yatsenko, Baas, Ponomarev, & Kropotov, 2010; Eichele, Rachakonda, Brakedal, Eikeland, & Calhoun, 2011; Ethridge et al., 2013; Antonakakis, Giannakakis, Tsiknakis, Micheloyannis, & Zervakis, 2013). This group-ICA creates scalp topography through the mixing matrix for each independent component shared across subjects. The current application overcomes (1) the problem of comparability of the ICA decomposition, (2) the stability problem of ICA (i.e. different temporal and spatial result at each application of ICA) when the temporal size (i.e. number of time-points) of the EEG signal is small (Jung et al., 2001). Also note that as reported by Montefusco-Siegmund et al. (2013), ICA can introduce phase distortions and may lead to biases in the metric computations. Nevertheless, these metrics (especially PIC and PsIC) are defined and operate within a narrow range of frequencies where we would expect fixed biases, with no effect on phase consistency. In addition, a successful combination of ICA and phase locking measures has already been reported by other studies (Phillips, Takeda, & Singh, 2012; Radüntz, Scouten, Hochmuth, & Meffert, 2015).

In the same adolescent twin EEG dataset as used previously for "classical" P300 analysis (van Beijsterveldt et al., 1998), we estimated independent components (ICs) by application of group ICA (Grin-Yatsenko et al., 2010; Eichele et al., 2011; Ethridge et al., 2013; Antonakakis et al., 2013). Next, we subjected these to a Continuous Wavelet Transform TF analysis (Torrence and Compo, 1998) for evoked and induced oscillatory responses (Bernat, Malone, Williams, Patrick, & Iacono, 2006; Hironaga and Ioannides, 2007; Jung et al., 2001; Zervakis et al., 2011). Finally, for each independent component, the PIC, PsIC, and SE time-frequency maps were separated into theta—θ (4–8 Hz), alpha—α low (8–10 Hz), α high (10–13 Hz), beta—β (13–30 Hz) and gamma—γ (30–45 Hz) frequencies in order to extract the specific response components, consistent with the notion that these frequencies reflect different aspects of cognitive processing (Klimesch, Sauseng, Hanslmayr, Gruber, & Freunberger, 2007). In doing so, the TF responses were averaged across time and across frequencies within a band, to obtain a single score per band per IC. We then carried out a variance decomposition model parsing individual variation in phase activity and energy into genetic and environmental variance components, to establish whether the PIC, PsIC and SE metrics are heritable traits and thus viable endophenotypes as the P300 amplitude for associated disease phenotypes. To our knowledge, this is the first attempt to study the genetics of source-level responses in the oddball task, which distinguishes between evoked and induced oscillatory responses.

2. Method

2.1. Subjects

The subjects were 213 pairs of 16-year-old Dutch twins (mean age = 16.18, S.D. = 0.55), including 39 monozygotic male (MZM), 52 monozygotic female (MZF), 36 dizygotic male (DZM), 38 dizygotic female (DZF), and 48 opposite sex dizygotic (DZOS) pairs, who were tested in the Psychophysiology Laboratory at the VU University Amsterdam, The Netherlands. Three subjects' tests were excluded because of technical difficulties. For 75.5% of all pairs zygosity was ascertained by being an opposite-sex twin pair, or based on DNA and/or blood markers. For the other pairs, zygosity was based on a standard set of questions (Boomsma, Koopmans, van Doornen, & Orlebeke, 1994). All participants signed informed consent and their parents when their age was below 18. The project was approved by the Ethical Board (METc) of the VU University Medical Centre.

2.2. Event related potentials

In the current study we analyze the ERP recordings for the visual oddball task, which were also used by the study of van Beijsterveldt et al. (1998). The oddball task consisted of a frequent stimulus (viz., non-targets), which was a line drawing of a dog for 100 epochs. The infrequent stimuli (viz., targets) consisted of a line drawing of a cat for 25 epochs and were presented randomly during the presentation of frequent stimuli to the subject. The stimulus duration was 100 ms and the time between stimuli varied quasi randomly from 1.5 to 2 s (mean = 1.75 s). Build-up time was <20 ms. A central fixation square was shown on the video monitor during the interstimulus interval. The instruction of eye movements was reduced by instruction to fixate on the current central square. Subjects were instructed to silently count of the infrequent target stimuli.

An 18-channel Nihon Kohden electroencephalograph (type EEG-4414A1K) was used for recording EEG-, EOG-, and ECG-signals. Monopolar brain (EEG), cardiac (ECG) and bipolar ocular (EOG) activity were measured by tin electrodes mounted in an electro cap at the scalp locations Fp1, Fp2, F7, F8, C3, C4, P3, P4, O1, O2, T5, and T6 according the 10–20 system (Jasper et al., 1958). Tin electrodes were placed at the canthus of each eye to record horizontal movements, horizontal EOG channel. To detect vertical movement, EOG was recorded from intra- and supra-orbital electrodes, in line with the pupil of the left eye, vertical EOG channel. Linked earlobes (A1, A2) were used as reference fed into separate high input impedance preamplifiers following the recommendations by (Pivik et al., 1993), which reduces the effects of possible imbalances in electrode impedance. The electrode impedance for EEG, ECG, and EOG was kept at or below 5 kΩ. A ground electrode was attached to FPz. For EEG, ECG, and EOG, conductive ECI electro-gel was used. Sampling rate of the AD-converter was set to 250 Hz and digital limitation of bandwidth was at frequency range of 0.03–30 Hz using a second order Butterworth band-pass filter.

2.3. Independent component analysis

The aim of ICA is to reveal independent sources of activity from different EEG signals and attempts to separate the corresponding generators of EEG rhythms. Methodologically, it attempts tries to estimate a set of spatial filters to invert the assumption of linear mixture sources at every electrode and recover the original sources, called independent components (ICs). Appendix A provides the definitions and assumptions of ICA.

2.4. Individual ICA

It has been shown that ICA is capable of reliably separating artifacts, such as blinking and lateral eye movement (Jung et al., 2000). The influence of ocular activity was detected and eliminated by decomposition of channels into ICs using extended Infomax algorithm (Delorme and Makeig, 2004; Jervis et al., 2007). ICs were determined in the combined EEG—EOG and ECG data. There were eighteen ICs on 125 trials for every individual, each trial with length 120 time-points. Ocular and cardiac artifacts were detected using the correlation values between trials of every IC with trials of the EOG (vertical and horizontal movements) and the ECG channel, respectively. Furthermore, the metrics of kurtosis and Rényi entropy estimated on every trial are used to support the correlation values. If the correlation and z-score values of metrics of at least 20% trials are larger than the threshold values of 0.7 for correlation and $\pm$1.64 for metrics (Escudero et al., 2011; Antonakakis et al., 2013), the IC is detected as artifact and removed (Escudero

et al., 2011; Dimitriadis et al., 2013; Antonakakis et al., 2013). After removing artifact components, the clean EEG was recovered via back projection of only the remaining components.

2.5. Group ICA

In our approach, we use ICA on concatenated artifact free channels in order to avoid the stability problem (Delorme et al., 2002; Grin-Yatsenko et al., 2010; Antonakakis et al., 2013) and compare characteristics between twin groups on ICs. The underlying assumption for such a group approach is that the way signals diffuse from the sources to the EEG channels is the same for all subjects in the group, so that there is a correspondence between signals from different subjects. This implies an assumption that the cortical localization of ICs is similar between all individuals, so that it is viable to implement the ICA for all groups. In theory, these assumptions do not exactly fit to EEG recorded from the scalp, but in practice the application of ICA for EEG analysis gives quite reasonable results (Onton and Makeig, 2006). Common cortical localization of ICs implies shared mixing matrix (Grin-Yatsenko et al., 2010; Eichele et al., 2011; Ethridge et al., 2013) that is used for the estimated representation of whitened brain activity into scalp topography and, as a consequence, common scalp maps for all subjects in each group or task considered.

In order to estimate the common mixing matrix, we maintained artifact-free channels from frontal, central, parietal, temporal and occipital scalp sites in both hemispheres (Fp1, Fp2, F7, F8, C3, Cz, C4, P3, Pz, P4, O1, O2, T5, and T6). Next, we concatenated the signals of all individuals. The concatenation involves all trials of the specific channels of twin groups in a common matrix with dimensions: 14 channels × 50400 time points × 110 trials. Dimensionality reduction was first performed preserving only the most dominant components with the most significant information (above 95% of total energy for all subjects) according to PCA (Delorme et al., 2002; Onton and Makeig, 2006; Dimitriadis et al., 2013; Antonakakis et al., 2013). The new dimensionality of the data was 10 principal components (PCs) × 50400 time (120 time points × 420 subjects) points × 110 trials. After the estimation of the application of group ICA, we maintained only those ICs that showed the highest eigenvalue, amplitude and structure similarity to P300.

2.6. Phase activity and spectrum energy

TF analysis is a powerful tool in the analysis of EEG signals (Bernat et al., 2006) and characterizes a signal in both the time and frequency domains simultaneously (Boashash, 1988). TF analysis was applied on ICs that reflect the brain sources generating the actual EEG signals during a specific task and may thus avoid the volume conduction effects. In addition, ICs are expected to partially decouple the complicated activity in the event related response (Iyer and Zouridakis, 2007; Zervakis et al., 2011).

For the TF analysis we employ the Continuous Wavelet Transform (CWT) (Daubechies, 1990). We adopted three measures of component consistency over trials in terms of phase, namely Spectrum Energy (SE), Phase inter-trial coherence (PIC) and Phase shift Inter-trial Coherence (PsIC) (Zervakis et al., 2011; Torrence and Compo, 1998). SE, PIC, and PsIC scores were examined for skewness of their population distribution, and data were log-transformed when needed. Details of the TF metrics are further presented in Appendix B.

2.7. Genetic analysis

We conducted an EEG twin study of target response, based on the phase and energy activity computed on the TF distributions of group-extracted ICs. The values of SE, PIC, and PsIC were averaged across frequencies for every brain rhythm of interest (θ, α-low, α-high, β, and γ). Alpha sub-bands are defined according to (Shackmana, McMenaminb, Maxwellc, Greischard, & Davidsone, 2010; Boersma et al., 2013). On the SE, PIC, PsIC for the 5 frequency bands of interest, we used structural equation model (SEM) with full information maximum likelihood (FIML) estimation for testing and estimating genetic and environmental contributions to individual variation in the outcome measures. Genetic models were fit to the data in the OpenMx package (Broker et al., 2011) available for free as a package in R (Ihaka and Gentleman, 1996).

Appendix C provides the most important details of the genetic models. In general, the quantitative genetic modeling paradigm follows a stepwise method of parameter reduction in a series of nested models that estimate mean and covariance association present in the data. The fit of data is expressed as minus two times the log of the likelihood of the fit of the model. We started with the most complex model fitting all correlations as free parameters for each sex and zygosity group, as well as freely estimated means, variances and betas for covariates age and sex. Subsequent models reduced the number of freely estimated parameters by equating correlations, means, and/or variances. These nested model strategy results in a monotonic reduction in likelihood. Twice the difference of log-likelihoods between nested models is asymptotically chi-square distributed with the number of free parameters lost as degree of freedom (df). By the rule of parsimony, nonsignificant differences result in the rejection of the more complex model.

2.8. Saturated model and testing (co) variances and means

We first fitted a saturated model to MZ and DZ data, in which we estimated separately for males and females the means and variances, for twin1, twin2 within pairs and for each zygosity ($model_1$). We then investigated whether the means and variances were equal across birth order (Twin1 = Twin2; $model_2$). Next, we tested equality of means and variances across zygosity (MZ = DZ; $model_3$). The equalities of means and variances across sex were examined by separate models (i.e., $M_{Males} = M_{Females}$; $model_4$ and $VAR_{Males} = VAR_{Females}$; $model_5$). Finally, correlations were equated across the sexes (rMZM = rMZF and rDZM = rDZF = rDZOS; $model_6$). All significance testing was FDR corrected. Significant effects (i.e., differences in means and variances) were retained in subsequent modeling.

This stepwise testing was performed for mean values of PIC, PsIC and SE for every IC, at every brain rhythm (theta, alpha low, alpha high and beta) for target stimuli. Due to the high number of tests, the p-values were adjusted using the Benjamini-Hochberg False Discovery Rate (FDR) adjustment (Benjamini and Hochberg, 1995).

2.9. Variance decomposition into genetic and environmental components

First, we fitted a univariate genetic model to test the significance of genetic and environmental components of variance. The phenotypic (P) variance was decomposed into additive genetic (A), common environmental (C: environmental influences shared by twins reared in the same family), and unique environmental (E; effects not shared between family members) variance (Boomsma et al., 2002). MZ twins share all genetic variance and DZ twins share on average 50%. Unique environmental influences are uncorrelated and also includes variance due to measurement error. All variance due to common environment is shared between MZ and DZ twins by definition. Significance of the variance components was assessed by dropping the component from the model and recording the increase in -2LL of the model.

3. Results

3.1. Average PIC, PsIC, and SE responses

Fig. 1 shows the topographic plots and the grand average ERPs of the four maintained ICs for PIC, PsIC, and SE. The topography of the evoked responses shows that IC1 reflected a strong P3 component that likely reflects the well-known activity from parietal sources. In addition, the early occipital responses are present in target and visual stimuli with weak P1 and P2 peaks. IC2 and IC4 reflected the bilateral early part of the visual oddball response. The grand average responses of IC3 reflected a more centrally oriented response. This functional distinction between a parietal (IC1) and more central response is well documented in the literature (Jung et al., 2001; Onton et al., 2006), and suggests that the ICA decomposition was successful in extraction these distinctive responses. After selecting these four ICs, we proceeded by calculating IC activity for each individual, performed a TF analysis for each, extracted PIC, PsIC, and SE in 5 frequency bands, and subjected these values to an analysis of individual differences.

The grand average TF images of phase activity (PIC and PsIC) and spectrum energy (SE) of target trials across all subjects are presented in Fig. 2. We show the TF responses in the widely studied frequency bands (θ, α low, α high, β and γ). Dashed lines indicate the boundaries for these bands. We first note that the three measures show distinct patterns in their respective TF images. For example, IC3 shows predominantly PsIC responses in θ band, whereas ICs 2 and 4 show PsIC responses in α low and α high bands. Therefore, independent components analysis was successful in separating the different types of responses, as identified by their evoked or induced nature. This further supports the assumption that different types of responses are generated by different neurobiological sources.

IC2 and IC4 show a very similar pattern of response, due to the fact that they reflect lateral homologues. Through the PIC metric, they reveal stronger evoked responses in lower α (ca. 200 ms). Both ICs reflect induced low and upper α responses near 180 ms and 600 ms post-stimulus, respectively. IC1 and IC3 on the other hand, show evidence for low amplitude evoked response (PIC) in the θ, low and high α bands around 150–400 ms post-stimulus. Concurrent induced responses (PsIC) are present for IC1 in the slow oscillations (θ) and additionally in upper alpha.

Within the five frequency bands, the responses could be averaged without loss of the main features (for example, IC2 PIC has clear responses in each of the β, lower α, and θ bands that are well separated among frequency bands). Averaging over the whole period can also be justified, even when responses are mainly restricted to 100–400 ms post-stimulus (individual differences were mostly determined by the strongest response period). The dark area outside the COI area of every TF representation indicates the region in which the edge effects of the CWT computation become unreliable, and was ignored.

3.2. Testing of group differences

Table 1 presents the parameters of compared models, only for statistically significant differences after FDR adjustment ($q = 0.05$). Most of the significant differences arise from the comparison of $model_3$ with $model_4$, which tests whether means and/or variances of males and females differed. We therefore retained sex differences in the mean in all further models. No significant differences were found in the correlations across the sexes, implying that only one MZ correlation (MZM with MZF) and one DZ correlation (DZM with DZF and DOS) sufficed.

3.3. Saturated model twin correlations

MZ and DZ correlations estimated by $model_6$ are shown in Fig. 3. Color-coding of Fig. 3 is according to significance of A and C according to ACE modeling results (see below). Twin correlations range from 0 to 0.6. For most variables, DZ correlations were lower than MZ correlations, indicating that genetic influences play a role.

3.4. ACE decomposition models

The statistical parameters of submodels fitting to ACE model for every frequency band, per IC and method are presented in Table S1 of the Supplementary material in 60 combinations (i.e., 5 frequency bands $\times$ 4 ICs $\times$ 3 methods). Each case investigated if it was possible to drop either A or C in 1df tests, or both A and C in a 2df test. Significance was FDR adjust at level $q = 0.05$ across 60 tests.

We summarize the results as follows. First, C was not significant in any combination of IC frequency and/or consistency metric. A was significant in 15 model combinations all for PsIC. In 11 cases, either A or C was significant in the 2df test, but the separate 1df tests remained undecided. A majority of those (i.e., 9) showed stronger effects for A than for C. The prevailing pattern of significant A effects, the absence of any significant C, and the bias in favor of A rather than C in the undecided cases suggest that the AE model may be the most appropriate model in our study. We decided to fit a single AE model to all combinations of IC, frequency, and variables in order to maximize comparability across the results. A color coding was created to illustrate the significant cases, i.e. dark orange if A is significant, light orange if A or C is significant with lower p-value for A, light blue if A or C is significant with lower p-value for C and no color if the case is not significant.

The heritability from the AE decomposition is shown in Fig. 4. The color on every bar follows the color-coding of the ACE significance in Fig. 3. Heritability of evoked response (reflected by PIC and SE metrics) was low (up to 35%) and remained not significant. Higher values of h^2 (24–55%) were found for the induced response (reflected by PsIC metric). Interestingly, the most consistent and strongest heritabilities were observed for IC1 and IC2, which showed minor P300 responses. These heritabilities also appear independent from peaks on the PsIC grand average of ICs, especially for β and γ bands. Overall, the most appropriate model fitting our analysis of genetic influences is the AE model as it also indicated for such similar purposes (Wright et al., 2001, 2002; Carlson and Iacono, 2006; Smit et al., 2006).

4. Discussion

This study aimed to investigate the heritability of individual differences in the brain response in a simple oddball task. Adolescent twins' time-locked EEG responses were parsed into ICs using group-based ICA, further parsed for evoked and induced oscillatory responses in the TF domains, which were then separated into well-known frequency bands. Group ICs are primarily localized on central, parietal and occipital brain areas (topographies of Fig. 1). The evoked oscillatory response mostly appears in α low frequency band. By contrast, the induced response and spectral energy are more prominent in θ, α low and α high. Next, the influences of genetic and environmental effects on frequency-specific responses were estimated. The AE model was the most suitable model for the majority of cases (Figs. 3 and 4). The resulting heritability values were consistently highest for the induced (phase-independent) oscillatory responses, and low for evoked responses.

The group ICA was successful in recovering some of the well-known components of the oddball task (Pfurtscheller and Lopes da Silva, 1999; Makeig et al., 2002; Kok, 2001; Polich, 2007; Zervakis

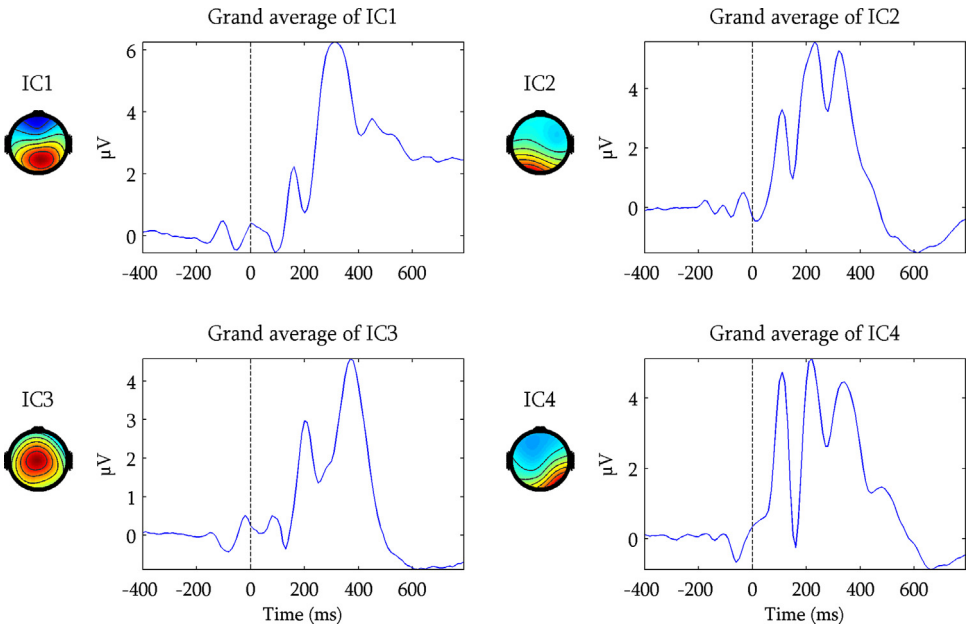

Fig. 1. Grand average of the single target trial for all the independent components. The coordinates of single trials are common for all the ICs. The distribution of color is common for the scalp topographies.

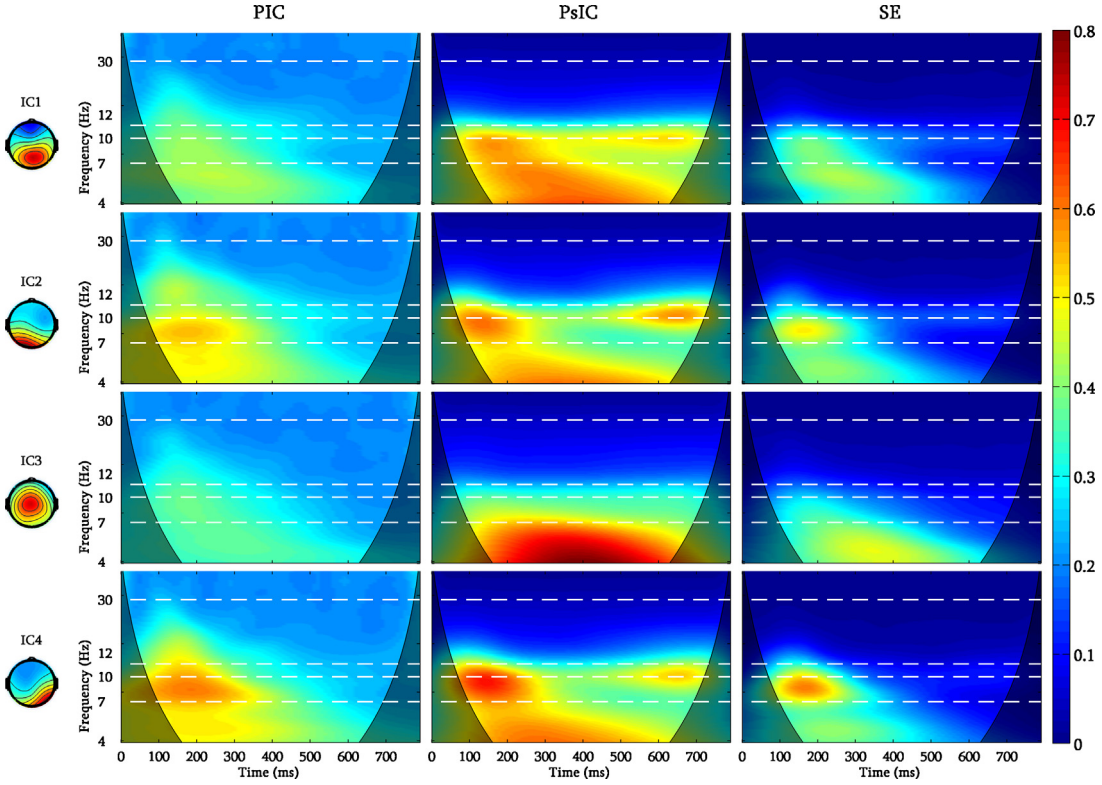

Fig. 2. Grand average of TF representations for phase activity (PIC), phase independent activity (PsIC) and spectrum energy (SE) of target mean trial. Thin black area represents area of COI. Scalp topographies were common for all subjects due to the estimation of common mixing matrix in the group-ICA. Color scale of between methods and ICs was common between groups per method. Dashed lines separate the investigated frequency bands, from which the final averaged values were extracted and were used to the genetic models. Topography maps in the first column reflect the strength of the corresponding common independent component projected on scalp electrodes. Shades of red indicate high values while shades of blue low values.

et al., 2011). The grand-average oscillatory responses (Fig. 2) show that ICs were specific in their response to the stimulus. IC1 clearly extracted the parietal stimulus-locked response as evidenced by the increase in evoked slow oscillations. The same component also reflected transient induced responses (PsIC) in the lower alpha and beta bands. IC3 reflected early positive peaks and sustained theta oscillations. Topography and signal waveforms of IC1 and IC3 are in correspondence with earlier ICA-based analysis of P300 activity (Jung et al., 2001; Onton and Makeig 2006) indicating that ICA applied on sets of single trials from event-related EEG experiments

Table 1
Statistically significant differences between submodels of saturated model of phase and energy activity of target single trial ICs.

IC	Band	Method	base	Vs	ep	−2LL	df	AIC	diffLL	diffdf	p
2	β	PsIC	$model_3$	$model_4$	25	573.51	417	-260.49	21.1	6	0.0007
2	β	SE	$model_3$	$model_4$	25	887.49	417	53.49	11.65	6	0.0385
4	β	PsIC	$model_3$	$model_4$	25	516.23	417	-317.77	27.46	6	0.0001

Model1 is the saturated model; model2 is the submodel of saturated model with equal means and variances between the twins per zygosity group (i.e., $Twin1_{MZ} = Twin2_{MZ}$); model3 with equal means and variances between zygosity groups (i.e., MZ = DZ); Models 4, 5, 6 with equal means, variances and correlations between sexes, respectively. Difference is significant with FDR adjustment at $q = 0.05$.

can enhance the information available from ERP analysis. Furthermore, the phase activities of both ICs are similar to corresponding experimental studies (Jung et al., 2001; Onton and Makeig, 2006; Zervakis et al., 2011; Ethridge et al., 2013). In addition to these experimental studies and their evoked oscillations, IC2 and IC4 also reflect early visual responses in occipital areas (N1), as well as late responses (N2, P3) in Fig. 2, while both ICs reflect PsIC oscillatory activity on lower α and θ bands. Shin et al., (2010) presented similar induced responses of ERP spectral perturbation on α and θ bands. Similar responses were also reported in the study of Zervakis et al. (2011), who focused on identifying and analyzing distinct responses in an auditory working memory paradigm.

The genetic analyses showed that, while ERP components generally have moderate to high heritability (van Beijsterveldt and van Baal, 2002; Anokhin, 2014), evoked oscillatory responses to the target stimulus (PIC, SE) showed low and non-significant heritability. This indicates that evoked potentials are inadequately captured by phase-locked oscillatory activity within the standard frequency bands. This outcome may partly support the findings of (Ethridge et al., 2013) who also investigated heritability of stimulus locked time-frequency analysis in an oddball task. In their study, the factors A and C could not be dropped simultaneously, although either could be dropped from low frequency bands (theta) to the beta bands. Note, however, that Ethridge et al. used a different approach in which heritability was estimated for each value of the TF spectral energy response to the oddball stimulus. The heritability scores were then clustered using PCA. Here, we first extracted ICs and computed multiple measures of the stimulus locked response, and subjected these to the genetic analysis. Gilmore, Malone, Iacono et al. (2010) showed that significant difference between the interclass correlations of MZ and DZ for the spectral energy of the β band, which is corroborates our finding for significant heritability for SE perturbations for IC1 in the β band (Fig. 3).

PsIC, on the other hand, showed significant evidence for additive genetic factors for many ICs and frequency bands, and consistently higher heritability than PIC or SE. This shows that not only evoked but also induced responses to targets in a simple cognitive task are heritable traits (Smit et al., 2007). Since induced responses are thought to reflect cognitive aspects different from evoked responses (Tallon-Baudry and Bertrand, 1996; Yordanova et al.,

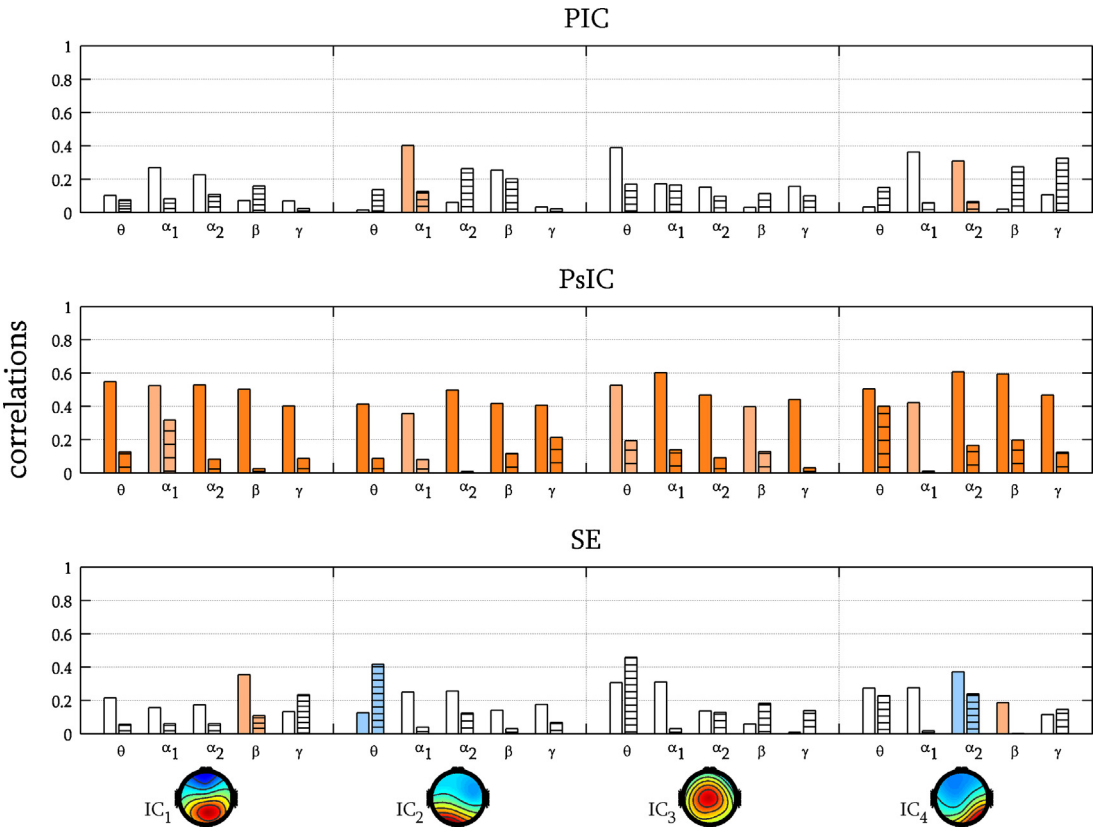

Fig. 3. Estimated correlations of target single trial between $Twin_1$ $Twin_2$ for MZ group and DZ group from model6 (assumption of equal correlation for sex differences). Model6 was the best fitting model according to its AIC value (smallest value in all cases). Frequency bands are listed in order from the left of every IC from theta to beta. Target is the type single trial. Dashed bars represent the DZ correlation. The bars are colored according to the significance level the variance decomposition models (Table S1). Dark orange: A was significant; light orange, dropping both A and C was significant in the 2df test, with the p-value for A lower in the 1df test; light blue: dropping both A and C was significant in the 2df test, with the p-value for C lower in the 1df test.

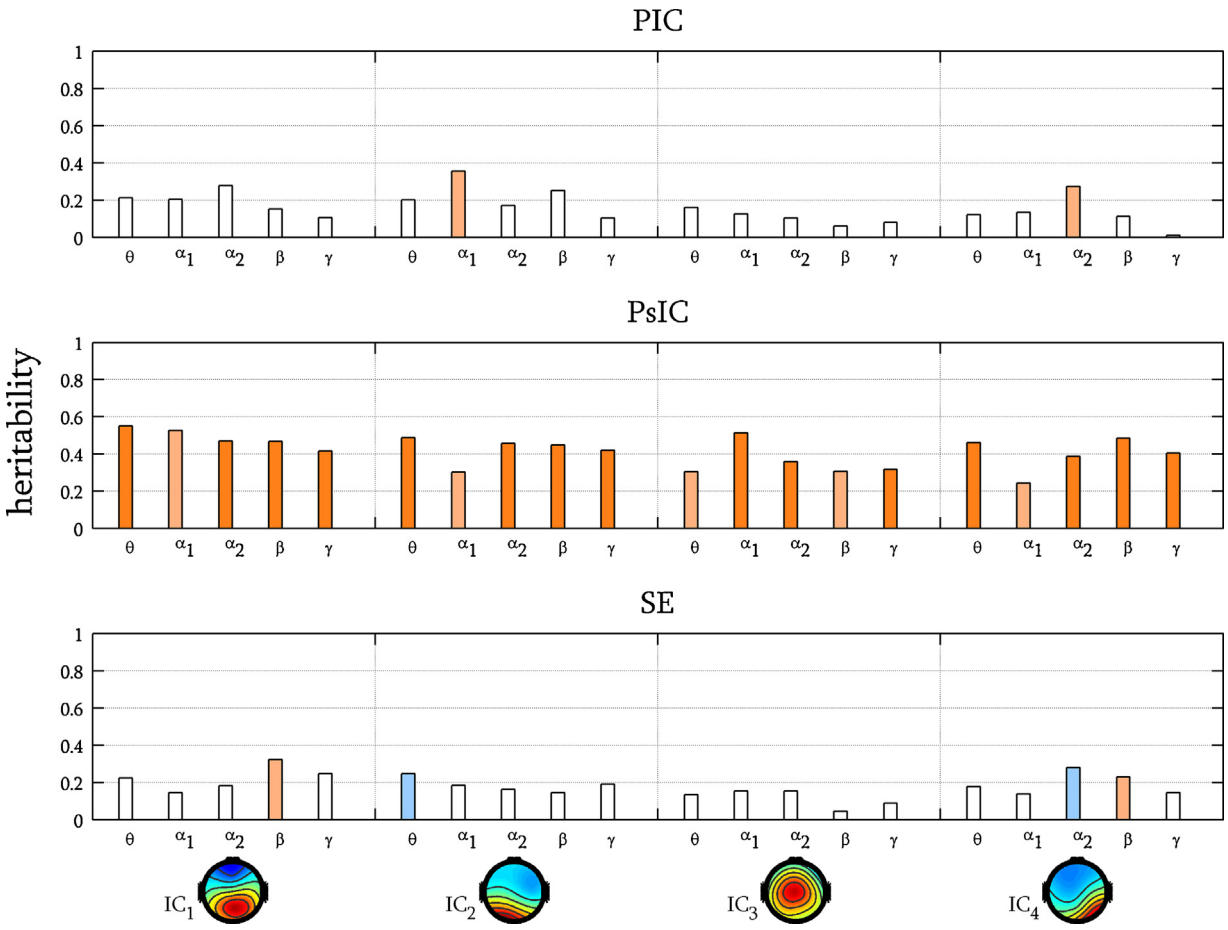

Fig. 4. Heritability (h^2) was tested in case of target phase and energy measures estimated by genetic model AE dropping common factor (C). C never reached significance ($p > .05$), with AE being the best fitting model for most of the decomposition. The separate vertical bars represent heritability in the frequency bands theta (θ), alpha low (α_1), alpha high (α_2), β and γ. The color coding is as in Fig. 3.

2001; Herrmann and Knight 2001), we conclude that the analysis of both types of responses is essential for a complete evaluation of the etiology of individual differences in the brain response to an oddball stimulus, and that the former could provide additional endophenotypes for human cognitive processing. Since induced responses are by definition phase independent, PsIC perturbations will not be visible in the standard ERP, and therefore reflect additional variability of cognitive processing (see also, Jensen and Mazaheri, 2010).

There is ample evidence of the involvement of the role of oscillations in cognitive processing (Klimesch, 1999; Jensen and Bonnefond, 2013) and their relation to task performance (e.g. working memory, visual cortex organization, attention binding effects). This evidence extends to induced responses (Tallon-Baudry et al., 1996; Makeig et al., 2002; Zervakis et al., 2011). For instance, IC 1, 2 and 4 showed clear alpha-band phase-independent activity (PsIC) and it may be related with the role of ongoing alpha oscillations in modulation of brain activity (Bonnefond and Jensen, 2012). The high heritability of alpha band suggests that induced responses may be endophenotypes for oddball task execution, which is known to be affected in psychiatric disease. For example, evoked (P300) responses to targets in auditory and visual oddball tasks are well established as endophenotypes in schizophrenia (Mathalon et al., 2000). Several genomic studies have investigated the brain response (including the P300 and delta and theta oscillations) as an endophenotype, but the reported effects are inconclusive (Callaway 1983; Bramon et al., 2006; Marco-Pallares et al., 2010). Finally, the γ band has been focus in recent endophenotype research, particularly in psychosis (Hall et al., 2006). Interestingly, the current study showed that PsIC in the γ band consistently showed the highest heritability across all ICs. Future investigations may investigate whether the correlation between γ band PsIC and psychosis is of a genetic nature.

Based on related literature, several suggestions can be made for the effect of specific genetic variants on evoked and/or induced responses to stimulus processing. Genetic variation in the DRD4 gene was found to increase theta activity—related to P300 amplitude—in response to a stimulus. A similar dependency was detected on COMT Val allele loading (Marco-Pallares, 2010). However, these genetic effects are at best subtle (Bramon et al., 2006). Other evidence correlating theta band responses to the target stimulus with various genetic polymorphisms includes the glutamate receptor gene (GRM8) (Chen et al., 2010), a gene-related rectifier channel demonstrated in a GWAS study at genome-wide significance level (Kang et al., 2012), the serotonin receptor gene HTR7 (Zlojutro et al., 2011), the corticotrophin releasing hormone receptor 1 gene (CRHR1) (Chen et al., 2010) and the association with KCNJ6. Note that these findings represent sporadic sources of evidence that need thorough replication and proper control for stratification effects (Ioannidis 2003; Munafó, 2006; Munafó and Flint 2004). A possible better avenue is the calculation of polygenic risk scores based on GWAS for disease phenotypes (e.g., Ripke et al., 2011) in large genomic/EEG samples to establish the effect of disease related genetic variants on the endophenotypes (see De Geus, 2010).

In conclusion, our study showed that source level EEG perturbations reveals evoked and induced oscillatory responses to a

simple oddball stimulus. Heritability analyses showed that evoked oscillatory responses were only weakly heritable. On the other hand, phase-independent induced responses were moderately to highly heritable. The proposed TF analysis extracts other sources of variation and complements the standard palette of ERP analysis by providing additional genetic information. The results of our study are consistent with other studies using the same or similar tasks that investigated heritability of oscillatory responses (Smit et al., 2008; Ethridge et al., 20131), but additionally used ICA to extract source level analysis and elaborated on the role of phase-independent induced oscillations. These results hold promise for future studies that investigate whether these TF responses show genetic overlap with related clinical and nonclinical phenotypes (De Geus, 2010; Krause et al., 2000; Doege et al., 2010).

Conflict of interest

The authors confirm that there is no a conflict of interest.

Acknowledgments

This research is partly supported by Greek NSRF2007-13Co-operation projects “AI-Care” and “ONCOSEED”, Twin-family database for behavior genetics and genomics studies (NWO 480-04-004), Genotype/phenotype database for behavior genetic and genetic epidemiological studies (NWO 911-09-032), BBR Foundation (NARSAD) 21668, and NWO/MagW VENI-451-08-026”.

Appendix A. Independent component aspects

The aim of ICA is to reveal independent sources of activity from different EEG signals and attempts to separate the corresponding generators of EEG rhythms. It tries to estimate a set of spatial filters that inverts the assumption of linear mixture sources at every electrode and recover the original sources, called independent components (ICs). Appendix A provides the definitions and assumptions of the ICA. These sources are approximated by $IC_{c_m}[n]$ and are decomposed from a set of single-trial EEG signals X by form:

$$S = WX,$$

where W called “unmixing” matrix that initially produces the set of EEG signals, X based on mutually independent sources$S$. Matrices$S$ and X at each time instant n are composed of the corresponding EEG signals, $X = [x_1[n] \ldots x_M[n]]^T$ and source entries $S = [s_1[n] \ldots s_M[n]]^T$, respectively for $m = 1, \ldots, M$ and $n = 1, \ldots, N$ where M indicates the number of channels on the scalp and N denotes the number of data points in the signal. In current study, matrix W is found by means of the Infomax algorithm, which is an iteration procedure that maximizes the mutual information between$S$. According to least squares estimation,

$$X = AS,$$

where the so-called “mixing” matrix $A = W^{-1}$ is the inverse matrix of W for $W = A^{-1}$ (or A^* where $*$denotes the pseudo-inverse). Furthermore,

$$X = \sum A_i S_i,$$

where A_i is the $i-$ th column of the matrix$A$ reflects the projection intensity of each IC back to the electrodes and form the basis of topographic mapping of this component. S_i - is the raw of S (i.e. time course of the independent component).

A valid application of ICA must be agree with assumptions such as: (1) distribution of potentials is not Gaussian; (2) generators of spatially separated components are temporally independent from each other; (3) summation of the electric currents induced by separate generators is linear at the scalp electrodes; (4) spatial distribution of components’ generators remains fixed across time. Unlike other EEG decomposition methods, such as Laplacian sharpening filters and PCA projection, ICA separates EEG sources with tangential as well as radial orientations and imposes independents instead of orthogonality in the time-courses of components. Thus, ICA decomposes the data into independent sources with dipolar scalp maps, without restrictive assumptions on head geometry or electrode locations (Makeig et al., 2004).

Appendix B. The time-frequency metrics

For TF analysis, we employ the Continuous Wavelet Transform (CWT) (Daubechies, 1990). The CWT has been developed as an important tool for time series analysis that contains non-stationary power (such as the EEG signal) at many different frequencies (Daubechies, 1990). Let $x_i[n]s$ represent the i_{th} trial ($n = 1, \ldots, N$) with time spacing δt and duration N data points ($N = 120$ in our case). In addition, we use the normalized complex-valued (non-analytic) Morlet wavelet, which has been extensively studied in EEG analysis (Demiralp, Ademoglu, Istefanopulos, Başar-Eroglu, & Başar, 2001) and given by form:

$$\psi(\eta) = \pi^{-\frac{1}{4}} e^{i\omega_0 \eta} e^{-\frac{\eta^2}{2}}$$

where the $e^{i\omega_0\eta}$ represents the Euler’s formula with η and ω_0 to be a non-dimensional time parameter and frequency, respectively. To approximate the CWT, the convolution between each single trial $x_i[n]$ and the $\psi(\eta)$ should be performed N times for each scale. The choice N convolutions is arbitrary and it could be reduced, say by skipping every other point in n (Torrence and Compo, 1998). We chose to work with the full length of epoch (N points), to provide sufficient resolution for the wavelet transform. The convolution theorem (Torrence and Compo, 1998) allows the implementation of all N convolutions simultaneously of $x_i[n]$ with consecutive scaled versions of a wavelet function $\psi(n)s$ by form:

$$X_i[k, n] = \sqrt{\frac{\delta t}{k}} \sum_{n'=0}^{N-1} x_{n'} \psi^* \left[\frac{(n' - n)\delta t}{k} \right]$$

The concept of scale is used as an alternative to frequency (Daubechies, 1990). Function ψ^* is the complex conjugate of function. $\psi X_i[k, n]$ is the complex-valued CWT of the i_{th} trial, $x_i[n]$, at specific frequency scale$k$. This is repeated for each trial starting at stimulus presentation. Three measures are derived in the CWT domain that reflects different forms of trial-to-trial consistency.

As a first measure of phased locked component consistency over trials in terms of phase, we calculate the normalized Spectrum Energy (SE) (Zervakis et al., 2011; Torrence and Compo, 1998) which reflects consistent amplitude of same phase over trials and is estimated by:

$$SE[k, n] = \frac{[\Sigma_i X_i[k, n]]^2}{\left[\max_{k,n} [\Sigma_i X_i[k, n]]^2 \right]}$$

SE emphasizes the evoked response of phase-locked nature consistent in all trials, which increases the energy of the mean (average) trial and is not associated with a random variational increase of just a few individual trails.

For the i_{th} trial, the phase shift is reflected as an exponential phase term in the TF representation. Phase inter-trial coherence (PIC) (Zervakis et al., 2011; Jervis et al., 2007; Tallon-Baudry et al.,

1996) detects patterns of oscillatory activity phase-locked across trials and given by:

$$\mathrm{PIC} = [k, n] = \frac{|\Sigma_i X_i[]k, n|}{\Sigma_i |X_i[]k, n|}$$

Viewing each complex value $X_i[k, n]$ in the TF maps as a vector in polar coordinates, PIC measures the uniformity of vector distribution (numerator) weighted by the relative amplitudes (denominator). The first part is similar to the Inter Trial Coherence (ITC) measure (Onton and Makeig, 2006; Tallon-Baudry et al., 1996). However, the ITC approach focuses on just the angles of complex vectors and projects the distribution of TF wavelet coefficients ($X_i[k, n]$) from multiple trials "i" to the unit circle with no respect to amplitude, altering them all in the complex plain (Martinez-Montes et al., 2008), whereas the PIC measure preserves the structure of the cloud of coefficients (phase and amplitude) so that it considers uniformity of the distribution weighted by the amplitude of phase-locked trials. In our view, determining the phase angle in low amplitude oscillations may introduce noise; therefore, the PIC forms a more representative measure than ITC for the characterization of phase-locked oscillatory activity in stimulus induced responses.

Different shifts of the same oscillatory signal from trial to trial induce only phase terms in the corresponding CWT coefficients. Thus, we can estimate the consistency of phase independent activity across trials using the energy distribution across trials through the so-called Phase shift Inter-trial Coherence (PsIC) (Zervakis et al., 2011):

$$PsIC[k, n] = \frac{\left[\Sigma_i |X_i[k, n]|^2\right]}{\max_{k,n}\left[\Sigma_i |X_i[k, n]|^2\right]}$$

The PsIC metric of induced responses exploits the energy distribution in individual trials instead of the signal's amplitude. Thus, it is based on the energy similarity among trials, which favors signals of the same frequency structure even if they are not synchronized in phase across trials. This metric eliminates phase effects and compares the inter-trial content of the trials based only on energy distribution normalized to the maximum value. In contrast, the SE metric reflects the energy of the average trial, which preserves only the synchronized signals across trials and eliminates every other activation. Notice that the PsIC computes the mean energy of individual signals in trials, whereas SE considers the energy of the mean signal over trials. Accordingly, random shifts (jitter) of the same signal over trials will result in signal suppression in the average signal (suppression of SE), but they will preserve the same power over trials and amplify the average energy of such a phase independent component (enhancement of PsIC).

Both SE and PIC maps reflect aspects of phase locking of oscillatory components over all trials, but they provide complimentary information. In particular, a non-oscillatory additive activity, or a partial phase-reset of large energy but only in a few trials, can cause an increase of the mean across trials and an increase of energy of the average signal (Martinez-Montes et al., 2008), which is captured by the SE measure. Nevertheless, since the PIC measure demonstrates the existence of phase-locked oscillatory activity consistent in all trials, this measure will not capture such kind of activity. Thus, the comparison of SE and PIC might be exploited in differentiating the character of phase-locked activity.

SE, PIC and PsIC can all be plotted as a two-dimensional TF map. A necessary point of caution related to the definition of SE, PIC and PsIC is that, due to the low temporal resolution at low frequencies, the wavelet coefficients present little variation in amplitude over the time course of the trial so that the specificity of measure's content (i.e. phase activity of P300 response) decreases. Hence, the reliability of this measure at very low frequencies must be handled with care, within the cone of influence (COI) for spectrum analysis of CWT coefficients (Torrence and Compo, 1998).

Appendix C. Genetic models

The genetic models consist of the (algebraic) specification of an expected means vector and covariance matrix based on free parameters, whose values are optimized. The covariance matrix of twin members holds the within family correlational structure. Starting at a sensible point in the free parameter space, the parameters in the means vector and covariance matrix are estimated. For each solution, the −2LL (minus two times the log-likelihood) is calculated as follows:

$$-2LL = -k\log(2\pi) + \log(|\Sigma|) + (X - M)\,\Sigma^{-1}(X - M)^T$$

where X contains the observed data for a family, M is the parameter based means estimate, Sigma is the estimated covariance matrix, and $|\cdot|$ denotes the trace. This function is applied to each row of data (twin pairs). Next, OpenMx iteratively searches through the parameter space minimizing −2LL -, thus maximizing the likelihood. The number *df* of the model is the total number of dependent observations minus the number of estimated parameters.

If free parameters are constrained at a specific value, a comparison of the two (nested) models A and B can be made by the so-called likelihood ratio test (LRT). In LRT, the −2LL between models is χ^2 distributed with the *df* equal to the difference in free parameters. If the resulting increases in −2LL is not significant; the simpler model is favored by rule of parsimony.

We tested whether there are differences in means, variances and correlations between twin zygosity groups and between males and females. This stepwise testing was performed for each parameter. Next, a variance decomposition was applied separating additive genetic (A), common environmental (C) and unique environmental effects (E), keeping the significant differences between sex or zygosity groups (in means, variances and correlations). Finally, significance of the factors A, C, and E was tested using variance decomposition models.

Appendix D. Supplementary data

Supplementary data associated with this article can be found, in the online version, at http://dx.doi.org/10.1016/j.biopsycho.2015.12.006.

References

Almasy, L., Porjesz, B., Blangero, J., Chorlian, D. B., O'Connor, S. J., Kuperman, S., et al. (1999). Heritability of event-related brain potentials in families with a history of alcoholism. *American Journal of Medical Genetics*, *88*, 383–390.

Anokhin, A. P. (2014). Genetic psychophysiology: advances, problems, and future directions. *International Journal of Psychophysiology*, *93*(2), 173–197.

Antonakakis, M., Giannakakis, G., Tsiknakis, M., Micheloyannis, S., & Zervakis, M. (2013). *Synchronization coupling investigation using ica cluster analysis in resting meg signals in reading difficulties*

Bates, A. T., Kiehl, K. A., Laurens, K. R., & Liddle, P. F. (2009). Low-frequency EEG: oscillations associated with information processing in schizophrenia. *Schizophrenia Research*, *115*, 222–230.

Benjamini, Y., & Hochberg, Y. (1995). Controlling the false discovery rate: a practical and powerful approach to multiple testing. *Journal of the Royal Statistical Society. Series B (methodological)*, *57*(1), 289–300.

Bernat, E. M., Malone, S. M., Williams, W. J., Patrick, C. J., & Iacono, W. G. (2006). Decomposing delta, theta, and alpha time-frequency ERP activity from a visual oddball task using PCA. *International Journal of Psychophysiology*, *64*, 62–74.

Boashash, B. (1988). Note on the use of the Wigner distribution for time frequency signal analysis. *IEEE Trans on Acoust Speech and Signal Processing*, *36*(9), 1518–1521.

Boersma, M., Smit, D. J. A., Boomsma, D. I., De Gues, E. J. C., Delemarre-van de Waal, H. A., & Stam, C. J. (2013). Growing trees in child brains: graph theoretical analysis of electroencephalography-derived minimum spanning tree in 5- and 7-year-old. Children reflects brain maturation. *Brain Connectivity*, *3*, 50–60.

Boomsma, D., Koopmans, J., van Doornen, L., & Orlebeke, C. (1994). Genetic and social influences on starting to smoke: a study of dutch twins and their parents. *Addiction*, *89*, 219–226.
Boomsma, D. I., Vink, J. M., van Beijsterveldt, T. C., de Geus, E. J., Beem, A. L., Mulder, E. J., Derks, E. M., Riese, H., Willemsen, G. A., Bartels, M., van den Berg, M., Kupper, N. H., Polderman, T. J., Posthuma, D., Rietveld, M. J., Stubbe, J. H., Knol, L. I., Stroet, T., & van Baal, G. C. (2002). Netherlands Twin Register: a focus on longitudinal research. *Twin Research*, *5*(5), 401–406.
Bramon, E., Dempster, E., Frangou, S., McDonald, C., Schoenberg, P., MacCabe, J. H., & Walshe. (2006). Is there an association between the COMT gene and P300 endophenotypes? *European Psychiatry*, *21*(1), 70–73.
Brockhaus-Dumke, A., Schultze-Lutter, F., Mueller, R., Tendolkar, I., Bechdolf, A., Pukrop, R., et al. (2007). Sensory gating in schizophrenia: P50 and N100 gating in antipsychotic-free subjects at risk, first-episode, and chronic patients. *Biological Psychiatry*, *64*(5), 376–384.
Broker, S., Neale, M., Maes, H., Wilde, M., Spiegel, M., Brick, T., Spies, J., Estabrook, R., Kenny, S., Bates, T., Mehta, P., & Fox, J. (2011). OpenMx: an open source extended structural equation modeling framework. *Psychometrika*, *76*(2), 306–317.
Callaway, E. (1983). Presidential address, 1982. The pharmacology of human information processing. *Psychophysiology*, *20*(4), 359–370.
Carlson, S. R., & Iacono, W. G. (2006). Heritability of P300 amplitude development from adolescence to adulthood. *Psychophysiology*, *43*, 470–480.
Chen, X., Simon, E. S., Xiang, Y., Kachman, M., Andrews, P. C., & Wang, Y. (2010). Quantitative proteomics analysis of cell cycle-regulated Golgi disassembly and reassembly. *Journal of Biological Chemistry*, *285*, 7197–7207.
Daubechies, I. (1990). The Wavelet transform, time-frequency localization and signal analysis. *IEEE Trans Inform Theory*, *36*, 961–1005.
David, O., Kilner, J. M., & Friston, K. J. (2006). Mechanisms of evoked and induced responses in MEG/EEG. *Neuroimage*, *31*, 1580–1591.
De Geus, E. J. (2010). From genotype to EEG endophenotype: a route for post-genomic understanding of complex psychiatric disease? *Genome Medicine*, *2*(9), 63.
Delorme, A., & Makeig, S. (2004). EEGLAB: an open source toolbox for analysis of single-trial EEG dynamics. *Journal of Neuroscience Methods*, *134*, 9–2.
Delorme, A., Makeig, S., Fabre-Thorpe, M., & Sejnowski, T. J. (2002). From single-trial EEG to brain area dynamics. *Neurocomputing*, *44–46*, 1057–1064.
Demiralp, T., Ademoglu, A., Istefanopulos, Y., Başar-Eroglu, C., & Başar, E. (2001). Wavelet analysis of oddball P300. *International Journal of Psychophysiology*, *39*, 221–227.
Dimitriadis, S. I., Laskaris, N. A., Simos, P. G., Micheloyannis, S., Fletcher, J. M., Rezaie, R., et al. (2013). Altered temporal correlations in resting-state connectivity fluctuations in children with reading difficulties detected via MEG. *Neuroimage*, *83*, 307–317.
Doege, K., Jansen, M., Mallikarjun, M., Liddle, E. B., & Liddle, P. F. (2010). How much does phase resetting contribute to event-related EEG abnormalities in schizophrenia? *Neuroscience Letter*, *481*(1), 1–5.
Ehringer, M. A., Rhee, S. H., Young, S., Corley, R., & Hewitt, J. K. (2006). Genetic and environmental contributions to common psychopathologies of childhood and adolescence: a study of twins and their siblings. *Journal of Abnormal Child Psychology*, *34*, 1–17.
Eichele, T., Rachakonda, S., Brakedal, B., Eikeland, R., & Calhoun, V. D. (2011). EEGIFT: group independent component analysis for event-related EEG data. *Computational Intelligence and Neuroscience*, *2011*, 65.
Ergen, M., Marbach, S., Brand, A., Başar-Eroglu, C., & Demiralp, T. (2008). P3 and delta band responses in visual oddball paradigm in schizophrenia. *Neuroscience Letters*, *440*(3), 304–308.
Escudero, J., Hornero, R., Abásolo, D., & Fernández, A. (2011). Quantitative evaluation of artifact removal in real magnetoencephalogram signals with blind source separation. *Annals of Biomedical Engineering*, *39*(8), 2274–2286.
Ethridge, L. E., Malone, S. M., Iacono, W. G., & Clementz, B. A. (2013). Genetic influences on composite neural activations supporting visual target identification. *Biological Psychology*, *92*(2), 329-4.
Ford, J. M., Roash, B. J., Hoffman, R. S., & Mathalon, D. H. (2008). The dependence of P300 amplitude on gamma synchrony breaks down in schizophrenia. *Brain Research*, *15*, 133–142.
Ford, J. M., Sullivan, E. V., Marsh, L., White, P. M., Lim, K. O., & Pfefferbaum, A. (1994). The relationship between P300 amplitude and regional gray matter volumes depends upon the attentional system engaged. *Electroencephalography and Clinical Neurophysiology*, *90*(3), 214–228.
Gilmore, C. S., & Fein, G. (2012). Theta event-related synchronization is a biomarker for a morbid effect of alcoholism on the brain that may partially resolve with extended abstinence. *Brain Behavioural*, *2*(6), 796–805.
Gilmore, C. S., Malone, S. M., Bernat, E. M., & Iacono, W. G. (2010). Relationship between the P3 event-related potential, its associated time-frequency components, and externalizing psychopathology. *Psychophysiology*, *47*(1), 123–132.
Gilmore, C. S., Malone, S. M., & Iacono, W. G. (2010). Brain electrophysiological endophenotypes for externalizing psychopathology: a multivariate approach. *Behaviour Genetics*, *40*, 186–200.
Gottesman, I. I., & Gould, T. D. (2003). The endophenotype concept in psychiatry: etymology and strategic intentions. *American Journal of Psychiatry*, *160*(4), 636–645.
Grin-Yatsenko, V. A., Baas, I., Ponomarev, V. A., & Kropotov, J. D. (2010). Independent component approach to the analysis of EEG recordings at early stages of depressive disorders. *Clinical Neurophysiology*, *121*(3), 281–289.
Hall, M. H., Schulze, K., Rijsdijk, F., Picchioni, M., Ettinger, U., & Bramon, E. (2006). Heritability and reliability of P300, P50 and duration mismatch negativity. *Behavior Genetics*, *36*, 845–857.
Herrmann, C. S., & Knight, R. T. (2001). Mechanisms of human attention: event-related potentials and oscillations. *Neuroscience and Biobehavioral Reviews*, *25*, 465–476.
Hironaga, N., & Ioannides, A. A. (2007). Localization of individual area neuronal activity. *Neuroimage*, *34*, 1519–1534.
Hyvärinen, A. (2001). Blind source separation by nonstationarity of variance: a cumulant-based approach. *IEEE Transactions on Neural Networks*, *12*(6), 1471–1474.
Ihaka, R., & Gentleman, R. (1996). R: a language for data analysis and graphics. *Journal of Computational and Graphical Statistics*, *5*(3), 299–314.
Ioannidis, J. P. (2003). Genetic association: false or true? *Trends in Molecular Medicine*, *9*(4), 135–138.
Iyer, D., & Zouridakis, G. (2007). Single-trial evoked potential estimation: comparison between independent component analysis and wavelet denoising. *Clinical Neurophysiology*, *118*, 495–504.
James, C. J., & Hesse, C. W. (2005). Independent component analysis for biomedical signals. *Physiological Measurement*, *26*(1), R15–R39.
Jasper, H. A. (1958). The ten-twenty system of the International Federation. *Electroencephalography and Clinical Neurophysiology*, *10*, 371–375.
Jensen, O., & Bonnefond, M. (2013). Prefrontal alpha- and beta-band oscillations are involved in rule selection. *Trends in Cognitive Sciences*, *17*(1), 10–12.
Jensen, O., & Mazaheri, A. (2010). Shaping: functional architecture by oscillatory alpha activity: gating by inhibition. *Frontiers in Human Neuroscience*, *4*, 186.
Jeong, J. (2004). EEG dynamics in patients with Alzheimer's disease. *Clinical Neurophysiology*, *115*, 1490–1505.
Jervis, B., Belal, S., Camilleri, K., Cassar, T., Bigan, C., Linden, D. E. J., et al. (2007). The independent components of auditory P300 and CNV evoked potentials derived from single-trial recordings. *Physiological Measurement*, *28*, 745–771.
Jung, T. P., Makeig, S., Humphries, C., Lee, T. W., McKeown, M. J., & Iragui, V. (2000). Removing electroencephalographic artifacts by blind source separation. *Psychophysiology*, *37*, 163–178.
Jung, T. P., Makeig, S., Westerfield, M., Townsend, J., Courchesne, E., & Sejnowski, T. J. (2001). Analysis and visualization of single-trial event-related potentials. *Human Brain Mapping*, *14*, 166–185.
Karrasch, M., Laine, M., Rinne, J. O., Rapinoja, P., Sinervä, E., & Krause, C. M. (2006). Brain oscillatory responses to an auditory-verbal working memory task in mild cognitive impairment and Alzheimer's disease. *Int J of Psychophysiology*, *59*, 168–178.
Klimesch, W. (1999). EEG alpha and theta oscillations reflect cognitive and memory performance: a review and analysis. *Brain Research Reviews*, *29*(2–3), 169–195.
Klimesch, W., Sauseng, P., Hanslmayr, S., Gruber, W., & Freunberger, R. (2007). Event related phase reorganization may explain evoked neural dynamics. *Neuroscience and Biobehavioral Reviews*, *31*(7), 1003–1016.
Kok, A. (2001). On the utility of P3 amplitude as a measure of processing capacity. *Psychophysiology*, *38*(3), 557–577.
Krause, C. M., Sillanmäki, L., Koivisto, M., Saarela, C., Häggqvist, A., & Laine, M. (2000). The effects of memory load on event-related EEG desynchronization and synchronization. *Clinical Neurophysiology*, *111*, 2071–2078.
Makeig, S., Debener, S., Onton, J., & Delorme, A. (2004). Mining event-related brain. *Trends in Cognitive Sciences*, *8*(5), 204–210.
Makeig, S., Westerfield, M., Jung, T. P., Enghoff, S., Townsend, J., & Courchesne, E. (2002). Dynamic brain sources of visual evoked responses. *Science*, *295*, 690–694.
Marco-Pallares, J., Nager, W., Kramer, U. M., Cunillera, T., Camara, E., & Cucurell, D. (2010). Neurophysiological markers of novelty processing are modulated by COMT and DRD4 genotypes. *Neuroimage*, *53*(3), 962–969.
Martinez-Montes, E., Cuspineda-Bravo, E. R., El-Deredy, W., Sanchez-Bornot, J. M., Lage-Castellanos, A., & Valdes-Sosa, P. A. (2008). Exploring event-related brain dynamics with tests on complex valued time-frequency representations. *Statistics in Medicine*, *27*, 2922–2947.
Mathalon, D. H., Ford, J. M., & Pfefferbaum, A. (2000). Trait and state aspects of P300 amplitude reduction in schizophrenia: a retrospective longitudinal study. *Biological Psychiatry*, *47*(5), 434–449.
Mazaheri, A., & Jensen, O. (2006). Posterior alpha activity is not phase reset by visual stimuli. *National Academy of Sciences of the USA*, *103*, 2948–2952.
Munafó, M. R., & Flint, J. (2004). Meta-analysis of genetic association studies. *Trends in Genetics*, *20*, 439–444.
Munafó, M. R. (2006). Candidate gene studies in the 21st century: meta-analysis, mediation, moderation. *Genes, Brain, and Behavior*, *5*, 3–8.
Nikulin V.V., Klaus Linkenkaer-Hansen K., Nolte G., Steven Lemm, Müller K.R., Llmoniemi R.J., Curio G., (2007): A novel mechanism for evoked responses in the human brain.
O'Connor, S., Morzorati, S., Christian, J., & Li, T. (1994). Heritable features of the auditory oddball event-related potential peaks, latencies, morphology and topography. *Electroencephalog and Clinical Neurophysiology*, *92*, 115–125.
Onton, J., & Makeig, S. (2006). Information-based modeling of event-related brain dynamics. *Progress in Brain Research*, *159*, 99–120.
Pfurtscheller, G., & Lopes da Silva, F. H. (1999). Event-related EEG/MEG synchronization and desynchronization: basic principles. *Clinical Neurophysiology*, *110*, 1842–1857.
Phillips, S., Takeda, Y., & Singh, A. (2012). Visual feature integration indicated by pHase-locked Frontal-parietal EEG signals. *Public Library Of Science*, *7*(3), e32502.

Pivik, R. T., Broughton, R. J., Coppola, R., Davidson, R. J., Fox, N., & Nuwer, M. R. (1993). Guidelines for the recording and quantitative analysis of electroencephalographic activity in research contexts. *Psychophysiology*, *30*, 547–558.
Polich, J., & Corey-Bloom, J. (2005). Alzheimer's disease and P300: review and evaluation of task and modality. *Current Alzheimer Research*, *2*(5), 515–525.
Polich, J. (2007). Updating P300: an integrative theory of P3a and P3b. *Clinical Neurophysiology*, *118*(10), 2128–2148.
Polich, J., & Herbst, K. L. (2000). P300 as a clinical assay: Rationale, evaluation, and findings. *International Journal of Psychophysiology*, *38*, 3–19.
Polich, J., & Bloom, F. E. (1999). P300, alcoholism heritability, and stimulus modality. *Alcohol*, *17*, 149–156.
Polich, J., & Ochoa, C. J. (2004). Alcoholism risk, tobacco smoking, and p300 event-related potential. *Clinical Neurophysiology*, *115*, 1374–1383.
Porjesz, B., & Begleiter, H. (2003). Alcoholism and human electrophysiology. *Alcohol Research & Health*, *27*(2), 153.
Porjesz, B., Rangaswamy, M., Kamarajan, C., Jones, K. A., Padmanabhapillai, A., & Begleiter, H. (2005). The utility of neurophysiological markers in the study of alcoholism. *Clinical Neurophysiology*, *116*(5), 993–1018.
Radüntz, T., Scouten, J., Hochmuth, O., & Meffert, B. (2015). EEG artifact elimination by extraction of ICA-component features using image processing algorithms. *Neuroscience Methods*, *243*, 84–93.
Ripke, S., et al. (2011). Schizophrenia psychiatric genome-wide association study (GWAS) consortium: genome-wide association study identifies five new schizophrenia loci. *Nature Genetics*, *10*, 969–976.
Shackmana, A. J., McMenaminb, B. W., Maxwellc, J. S., Greischard, L. L., & Davidsone, R. J. (2010). Identifying robust and sensitive frequency bands for interrogating neural oscillations. *Neuroimage*, *51*(4), 1319–1333.
Shah, N. M., Pisapia, D. J., Maniatis, S., Mendelsohn, M. M., Nemes, A., & Axel, R. (2004). Visualizing sexual dimorphism in the brain. *Neuron*, *43*, 313–319.
Shin, Y. W., Krishnan, G., Hetrick, W. P., Brenner, C. A., Shekhar, A., Malloy, F. W., et al. (2010). Increased temporal variability of auditory event related potentials in schizophrenia and schizotypal. *SPersonality Disorder Schizophrenia Research*, *124*(1–3), 110–118.
Smit, D. J., Boersma, M., van Beijsterveldt, C. E., Posthuma, D., Boomsma, D. I., Stam, C. J., & de Geus, E. J. C. (2010). Endophenotypes in a dynamically connected brain. *Behavior Genetics*, *40*, 167–177.
Smit, D. J., Posthuma, D., Boomsma, D. I., & de Geus, E. J. (2007). Heritability of anterior and posterior visual N1. *International Journal of Phychosiology*, *66*(3), 196–204.
Smit, D. J., Stam, C. J., Posthuma, D., Boomsma, D. I., & de Geus, E. J. (2008). Heritability of small world networks in the brain: a graph theoretical analysis of resting-state EEG functional connectivity. *Human Brain Mapping*, *29*, 1368–1378.
Smit, D. J., van Ent, D., de Zubicaray, G., & Stein, J. L. (2012). Neuroimaging and genetics: exploring, searching, and finding. *Twin Research and Human Genetics*, *15*, 267–272.
Smit, D. J. A., Posthuma, D., Boomsma, D. I., & de Geus, E. J. C. (2006). Genetic contribution to the P3 in young and middle-aged adults. *Twin Research and Human Genetics*, *10*(2), 335–347.
Soltez, F., Szucs, D., Leong, V., White, S., & Goswami, U. (2013). Differential entrainment of neuroelectric delta oscillations in developmental dyslexia. *Public Library Of Science*, *8*(10), e76608.
Tallon-Baudry, C., Bertrand, O., Delpuech, C., & Pernier, J. (1996). Stimulus specificity of phase locked and non-phase-locked 40Hz visual responses in human. *Journal of Neuroscience*, *16*, 4240–4249.
Torrence, C., & Compo, G. P. (1998). A practical guide to wavelet analysis. *Bulletin of the American Meteorological Society*, *79*(1), 61–78.
Ucles, P., Mendez, M., & Garay, J. (2009). Low-level defective processing of non-verbal sounds in dyslexic children. *Dyslexia*, *15*(2), 72–85.
van Beijsterveldt, C. E., Molenaar, P. C. M., de Geus, E. J. C., & Boomsma, D. (1998). Individual differences in P300 amplitude: a genetic study in adolescent twins. *Biological Phychology*, *47*, 97–120.
van Beijsterveldt, C. E., & van Baal, G. C. (2002). Twin and family studies of the human electroencephalogram: a review and a meta-analysis. *Biological Psychology*, *61*, 111–138.
van Dongen, J., Slagboom, P. E., Draisma, H. H., Martin, N. G., & Boomsma, D. I. (2012). The continuing value of twin studies in the omics era. *Nature Reviews. Genetics*, *13*(9), 640–653.
Wright, M. J., Hansell, N. K., Geffen, G. M., Geffen, L. B., Smith, G. A., & Martin, N. G. (2001). Genetic influence on the variance in P3 amplitude and latency. *Behavior Genetics*, *31*(6).
Wright, M. J., Luciano, M., Hansell, N. K., Geffen, G. M., Geffen, L. B., & Martin, N. G. (2002). Genetic sources of covariation among P3(00) and online performance variables in a delayed-response working memory task. *Biological Psychology*, *61*, 183–202.
Yordanova, J., Kolev, V., & Polich, J. (2001). P300 and alpha event-related desynchronization (ERD). *Psychophysiology*, *38*, 143–152.
Zervakis, M., Michalopoulos, K., Iordanidou, V., & Sakkalis, V. (2011). Intertrial coherence and causal interaction among independent EEG components. *Journal of Neuroscience Methods*, *197*, 302–314.
Zlojutro, M., Manz, N., Rangaswamy, M., Xuei, X., Flury-Wetherill, L., Koller, D., Bierut, L. J., Goate, A., Hesselbrock, V., Kuperman, S., Nurnberger, J., Jr, Rice, J. P., Schuckit, M. A., Foroud, T., Edenberg, H. J., Porjesz, B., & Almasy, L. (2011). Genome-wide association study of theta band event-related oscillations identifies serotonin receptor gene HTR7 influencing risk of alcohol dependence. *American Journal of Medical Genetics B Neuropsychiatric Genetics*, *156B*, 44–58.